

# Hydrothermal synthesis and characterization of fluorine & manganese co-doped PZT based cuboidal shaped powder

**H. Nawaz, M. Shuaib, M. Saleem, A. Rauf and A. Aleem**

Institute of Industrial Control Systems, P.O. Box 1398, Rawalpindi, Pakistan

E-mail: rhn.qau@gmail.com

**Abstract.** Cuboidal shaped PZT powder particles based composition  $\text{Pb}_{0.89}(\text{Ba}, \text{Sr})_{0.11}(\text{Zr}_{0.52}\text{Ti}_{0.48})\text{O}_3$  co-doped with 1 mol% manganese and 2 mol% fluorine was prepared through hydrothermal route. 200-250nm size cuboidal particles were observed under FE-SEM. XRD technique revealed that the perovskite type ceramic structure has a dominant rhombohedral phase. The resultant powder particles were then spray dried, uniaxially pressed and sintered at different temperatures to achieve maximum theoretical density. 98% density was obtained in the pellets at a sintering temperature of 1190°C with an average grain size of 1-3µm. The electrical properties of sintered samples were also measured before and after poling to evaluate the effect of dopants on piezoelectric properties.

## 1. Introduction

The composition of piezoelectric materials can be tailored to achieve properties suited for many applications such as medical imaging, dielectrics, thermal detectors, microwave resonators and transducers [1]. Out of these piezoelectrics, perovskite type, lead zirconate titanate (PZT) are of particular interest. Although pure PZT ceramics are not often used, their electrical properties can be modified by the addition of dopants. The dopants are classified into two classes i.e., donors and acceptors. The donor dopants induce soft piezo character i.e., increase dielectric constant & charge coefficient  $d_{33}$ . The excess of positive charge in soft PZT is compensated by lead vacancies. Whereas the acceptor dopants give rise to hard PZTs i.e., lower dielectric constant and  $d_{33}$ . These type of dopants induce oxygen vacancies in the system [2]. The effect of co-doping on the properties of Piezoceramics has also been studied extensively. Guiffard et al. have reported that the Mn-F co-doped PZT, prepared through co-precipitation method, have high mechanical quality factor  $Q_m$  and better electromechanical & dielectric characteristics [3].

The PZT ceramic powders can be prepared by mechanical alloying, co-precipitation and hydrothermal routes. However, the powder particles prepared via hydrothermal route is advantageous in many prospects including chemical homogeneity and lower sintering temperature [4]. As a result lead volatilization is minimized during sintering process and sintered product is expected to have uniform chemical composition.

According to best of our knowledge, (Mn,F) co-doped PZTs have not yet been synthesized through hydrothermal route. This study focuses on the structural and electrical characterization of the hydrothermally synthesized composition  $[\text{Pb}_{0.89}(\text{Ba}, \text{Sr})_{0.11}(\text{Zr}_{0.52}\text{Ti}_{0.48})\text{O}_3]$  co-doped with 1 mol% manganese and 2 mol% fluorine.



## 2. Materials

The materials used in this study includes Iso-Propanol (99.5%, BDH), Lead Nitrate (99%, Fisher), Titanium (IV) isopropoxide (99.5%, Fluka), Zirconium (IV) n-propoxide (70%, Alfa Aesar), Barium Acetate (99%, Riedel-de Haen), Strontium Acetate (99%, Alfa Aesar), Lead Fluoride (99.5%, Alfa Aesar), Manganese Acetate (99%, Acros organics), Poly Vinyl Alcohol (Merck), DOLOPIX (PC 67, ZS Chimmer & Schwarz), Acetic Acid (Sigma Aldrich) and KOH (Merck)

## 3. Experimental

A solution of Zirconium n-propoxide and Titanium isopropoxide was prepared in Iso-Propanol. The solution was co-precipitated in water and filtered. The filtrate was mixed with the stoichiometric amounts of Lead Nitrate, Barium Acetate, Strontium Acetate, Lead Fluoride and Manganese Acetate. Distilled water was then added upto  $3/4^{\text{th}}$  of the vessel and the pH of the system was raised to 14 using KOH pellets. The prepared solution was loaded into the chamber of R-201 type reactor system and a hydrothermal treatment was carried out at 260 °C under auto-generated pressure. After completion of reaction, the synthesized powder was filtered and washed twice with distilled water and once with dilute acetic acid to remove unreacted Lead Acetate and again with distilled water. Finally, the filtrate was dried in an oven at 100 °C.

The powder particles, thus obtained, were mixed with binder (PVA) and dispersant (DOLOPIX) and spray dried. The resulting powder was uniaxially pressed in the form of pellets and sintered at different temperatures to optimize the density.

## 4. Characterization

Size and morphology of the powder particles was characterized using a *Quanta-450* FEG-SEM technique. The structural characterization of the powder samples was carried out by *JEOL JDX9C* X-ray diffractometer using  $\text{CuK}\alpha$  ( $\lambda = 1.54056 \text{ \AA}$ ) radiations. The samples were scanned from  $20^\circ$  -  $80^\circ$  with a scan rate of  $1^\circ$  per second at a current and voltage ratings of 35mA and 30KV, respectively. The morphology of the sintered pellets was observed through *JSM-5910 LV*, JEOL Scanning Electron Microscopy (SEM), whereas the density was measured using Archimedes' Principle. For the electrical measurements, sintered samples were electroded with silver paste on both sides and fired at 700 °C. The samples were then poled with an applied field of 3KV/mm in a silicone oil bath at 120 °C. Electrical properties such as capacitance, piezoelectric coefficient ( $d_{33}$ ) and mechanical quality factor ( $Q_m$ ) were measured using *7600 Precision* LCR meter, *PM-300* Piezo Meter and *TA-2000* respectively.

## 5. Results and discussion

### 5.1. X-ray diffraction analysis

Figure 1 shows the typical XRD pattern of provskite PZT based powder particles along with miller indices for each peak. Mn addition led to the formation of rhombohedral phase instead of tetragonal phase as depicted by (200) peak instead of (211) which is a typical behaviour of manganese doped PZT systems [5-6].

Possible explanation for phase change may be related to the ionic state of manganese ( $\text{Mn}^{+4}$ ,  $\text{Mn}^{+2}$  and  $\text{Mn}^{+3}$ ) and its location in the perovskite structure where it substitutes the B-site ion.  $\text{Mn}^{+2}$  assumes high spin states  $t_{2g}^3 e_g^2$  ( $d_5$ ) and  $\text{Mn}^{+3}$   $t_{2g}^3 e_g^1$  ( $d_4$ ) as  $\text{O}^{2-}$  is a weak ligand. The presence of symmetrical spin state  $t_{2g}^3 e_g^2$  suggests that  $d^4$  electron state of  $\text{Mn}^{+3}$  ion makes it a Jahn–Teller ion along with the generation of Jahn–Teller distortion [7].

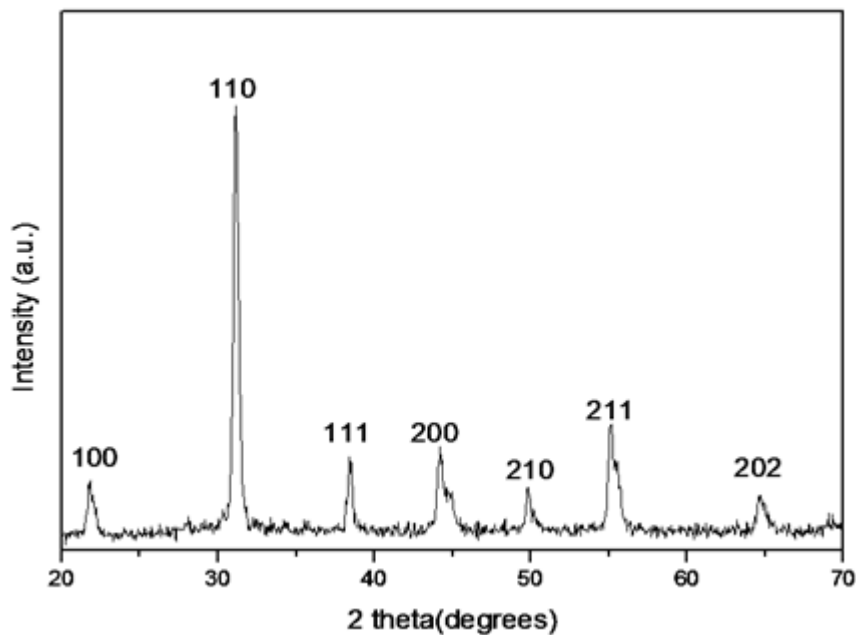


**Figure 1.** XRD pattern of  $\text{Pb}_{0.89}(\text{Ba}, \text{Sr})_{0.11}(\text{Zr}_{0.52}\text{Ti}_{0.48})\text{O}_3$  co-doped with 1 mol% manganese and 2 mol% fluorine powder particles

Splitting of orbitals from the Jahn-Teller effect for  $\text{Mn}^{+3}$  ion has been shown in Figure 2. The Figure shows that  $d_z^2$  orbital is occupied by none of the d-electron which results in higher electron density in xy-plane as compared to z-direction. Thus the electrostatic attraction between  $\text{Mn}^{+3}$  and  $\text{O}^{2-}$  ligands experiences low shielding effect in z-direction as compared to that of xy-plane. This decreases the c/a ratio in the unit cell so rhombohedral phase is exhibited by the perovskite type structure with Mn addition.

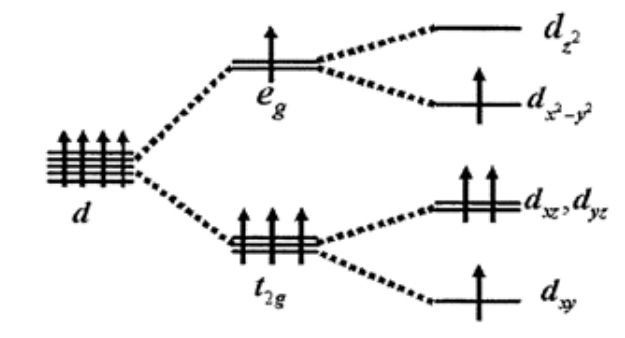


**Figure 2.** Splitting of orbitals of  $\text{Mn}^{+3}$  ion from the Jahn-Teller effect

### 5.2. Morphological analysis

The morphological analysis of the synthesized powder and sintered pellets was carried out using FE-SEM and SEM respectively (Figure 3). Figure 3(a) & (b) show the cuboidal geometry of powder particles having size of 200-250 nm size. The uniformity in the geometry is a characteristic feature of hydrothermal route. Such powder particles lead to a uniform grain growth during sintering [4] as shown in Figure 3 (c) & (d). Fully dense structure with 1-2 $\mu\text{m}$  grain size was observed in the sintered pellets. Smaller grain size may be attributed to the hydrothermal processing which resulted fine powder particles. The grain size may also be correlated with the dopant addition. During sintering the build-up of Mn at grain boundaries restricts the grain growth [8] however, on the other hand the addition of Fluorine leads to  $\text{PbO}$  and/or  $\text{PbF}_2$ -rich secondary phases causing an increase in the density along with grain growth promotion [9,10].

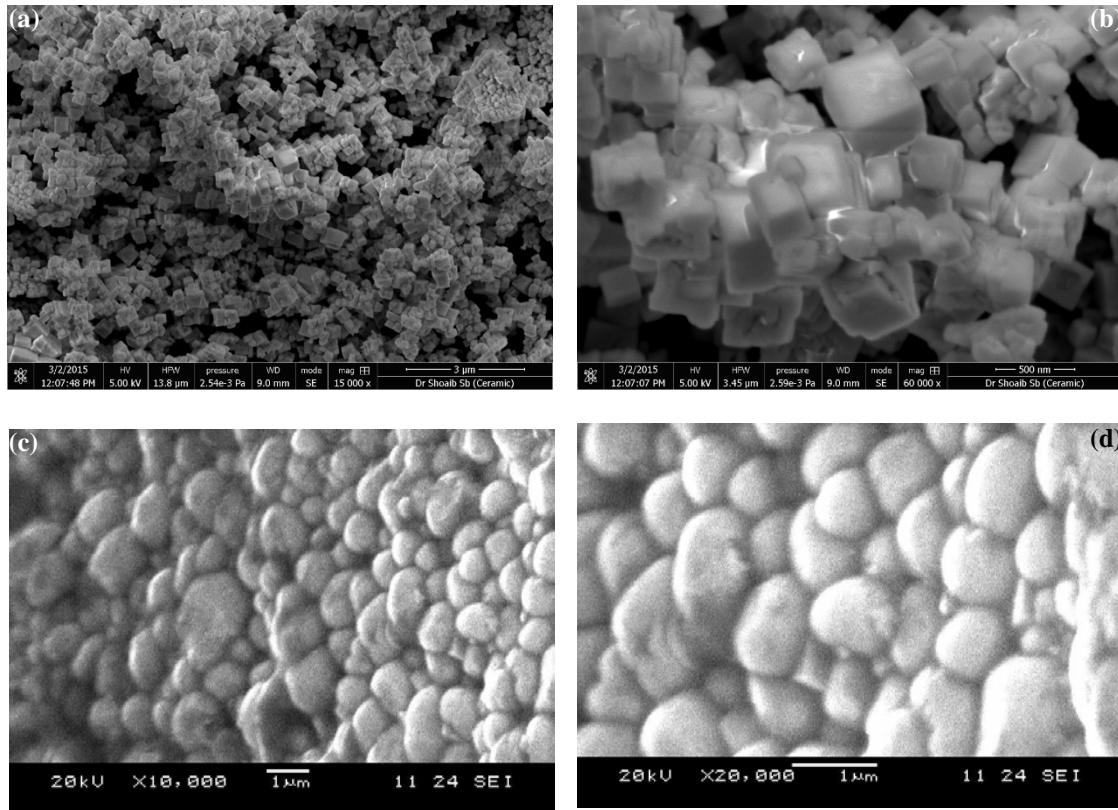


**Figure 3.** (a & b) FE-SEM micrographs of synthesized PZT powder showing cuboidal particles, (c & d) SEM images of fractured PZT pellets showing highly dense structure

### 5.3. Density measurement

The powder particles were pressed and sintered at different temperatures from 1150-1200 °C for 2 hours to optimize the density. Figure 4 shows the variation of density as a function of temperature. It can be seen from the graph that >98% of the theoretical density was achieved at 1190 °C.

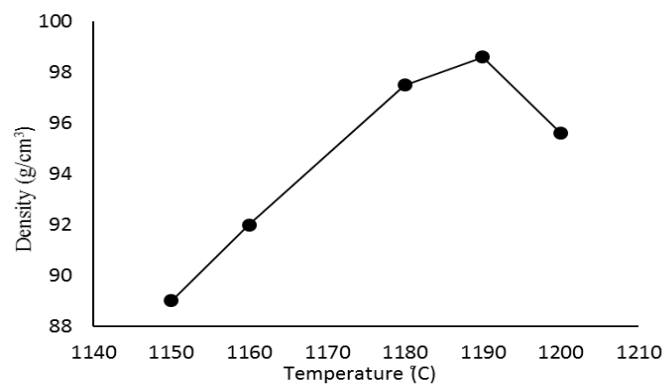


**Figure 4.** Influence of sintering temperature on densification at constant stay time (2 hours) and heating rate (5 °C/min)

### 5.4 Electrical properties

The electrical properties dielectric constant  $K_{33}^T$ , dielectric loss factor  $\tan\delta$ , piezoelectric coefficient  $d_{33}$ , the electromechanical coupling coefficient  $k_{33}$  and the mechanical quality factor  $Q_m$  of the samples have been listed in Table 1. The properties listed in the table are in good agreement to the previous studies [3]. The piezoelectric activity has been improved to a great deal due the presence of dopants.

**Table 1.** Electrical properties of sintered samples before and after poling

Before Poling				After Poling				
$K_{33}^T$	$R (K\Omega)$	$\tan\delta$	$K_{33}^T$	$R(K\Omega)$	$\tan\delta$	$k_{33}(\%)$	$Q_m$	$d_{33}(pC/N)$
1150	4.5	0.026	1280	3.1	0.018	56	320	280

The combined effect of manganese and fluorine imparts unique properties in the system. Fluorine is expected to substitute for oxygen defects caused by the manganese doping, making possible to pole PZT system at 3KV/mm [11]. On the other hand, Mn addition lowers the saturation field of perovskite type ferroelectrics by decreasing the  $c/a$  ratio of crystal lattice and thus increases electromechanical coupling coefficient. The trivalent B site ion ( $Mn^{+3}$ ) also forms dipoles with oxygen atoms which gives rise to “clamping effect” as a result the wall movement of ferroelectric domain is restricted [12]. This ultimately increases the mechanical quality factor.

### 6. Conclusion

The effect of co-doping of 1 mol% manganese and 2 mol% fluorine on hydrothermally prepared  $Pb_{0.89}(Ba, Sr)_{0.11}(Zr_{0.52}Ti_{0.48})O_3$  was evaluated in the present study. Powder particles of 250-300 nm size with a cuboidal morphology were observed under FE-SEM. XRD analysis of powder particles confirmed the formation of rhombohedral phase in the PZT perovskite structure. It was found out that more than 98% theoretical density is achieved at a sintering temperature of 1190 °C, for the studied composition. The grain size of 1-2um was observed in the sintered pellets. Moreover the electrical properties such as the piezoelectric coefficient  $d_{33}$ , the electromechanical coupling coefficient  $K_{33}$  and the mechanical quality factor  $Q_m$  increase by the addition of dopants.

### 7. References

- [1] Thomann H and Heywang W 1984 Annu. Rev. Mat. Sci. 14 27-47
- [2] Berlincourt D 1992 J. Acoust. Soc. Am 91 3034-40
- [3] Guiffard B, Boucher E, Lebrun L and Guyomar D 2007 Mat. Sci. and Engg. B 137 272-7
- [4] Maria T, Christian C, Anne L and Bernard T 1999 J. Euro. Cer. Soc. 19 1023-6
- [5] Ibrahim S, Hanna F and Marei L 2003 Egypt. J. Sol. 26 139-50
- [6] Hou Y, Zhu M, Gao F, Wang H, Wang B, Yan H and Tian C 2004 J. Am. Ceram. Soc. 87 847-50
- [7] Porter B and Harvey K 1972 Introduction to Physical Inorganic Chemistry: (Addison-Wesley)
- [8] Izaki T, Haneda H, Watanabe A, Uchida Y, Tanaka J and Shirasaki S 1992 Jpn. J. Appl. Phys. 31 3045
- [9] hiang S, Nishioka M, Fulrath R and Pask 1981 J. Ceram. Bull. 60 484
- [10] Ohtaka O, Von DerMühl R and Ravez J 1995 J. Am. Ceram. Soc. 78 805
- [11] Eyraud L, Eyraud P, Audiger D, and Claudel R 1995 Ferroelectric. 175 241–50
- [12] Kamiya T, Suzuki T, Tsurumi T and Daimon M 1992 Jpn. J. Appl. Phys. 31 3058-60